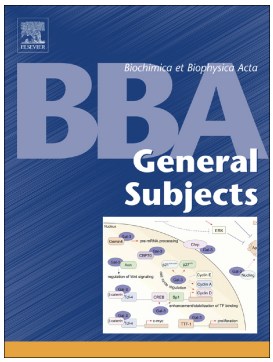

PAXgene fixation enables comprehensive metabolomic and proteomic analyses of tissue specimens by MALDI MSI

Christian Urban, Achim Buck, Jens T. Siveke, Florian Lordick, Birgit Luber, Axel Walch, Michaela Aichler

PII: S0304-4165(17)30326-4
DOI: doi:10.1016/j.bbagen.2017.10.005
Reference: BBAGEN 28959

To appear in:

Received date: 2 August 2017
Revised date: 28 September 2017
Accepted date: 8 October 2017

Please cite this article as: Christian Urban, Achim Buck, Jens T. Siveke, Florian Lordick, Birgit Luber, Axel Walch, Michaela Aichler , PAXgene fixation enables comprehensive metabolomic and proteomic analyses of tissue specimens by MALDI MSI. The address for the corresponding author was captured as affiliation for all authors. Please check if appropriate. Bbagen(2017), doi:10.1016/j.bbagen.2017.10.005

PAXgene fixation enables comprehensive metabolomic and proteomic analyses of tissue specimens by MALDI MSI

Christian Urban[1‡], Achim Buck[1‡], Jens T. Siveke[2,3], Florian Lordick[4], Birgit Luber[5], Axel Walch[1*] and Michaela Aichler[1*]

[‡]These authors contributed equally to this work.

Author affiliations:
[1]Research Unit Analytical Pathology, Helmholtz Zentrum München, Neuherberg, Germany
[2]German Cancer Consortium (DKTK) and German Cancer Research Center, DKFZ, Heidelberg, Germany
[3]Division of Solid Tumor Translational Oncology, German Cancer Consortium (DKTK), Partner Site Essen, West German Cancer Center, University Hospital Essen, Germany
[4]University Cancer Center Leipzig (UCCL), University Medicine Leipzig, Leipzig, Germany
[5]Institut für Allgemeine Pathologie und Pathologische Anatomie, Technische Universität München, Klinikum rechts der Isar, München, Germany

Author emails:
christian.urban@helmholtz-muenchen.de
achim.buck@helmholtz-muenchen.de
j.siveke@dkfz-heidelberg.de
florian.lordick@medizin.uni-leipzig.de
birgit.luber@tum.de
axel.walch@helmholtz-muenchen.de
michaela.aichler@helmholtz-muenchen.de

*Corresponding authors:
Axel Walch, Michaela Aichler, Research Unit Analytical Pathology, Helmholtz Zentrum München, Ingolstädter Landstr. 1, 85764 Neuherberg, Germany; E-mail: axel.walch@helmholtz-muenchen.de, michaela.aichler@helmholtz-muenchen.de; Phone: +49 89 3187-2739; Fax: +49 89 3187 3349

Competing Financial Interests:
The authors declare no competing financial interests.

Abstract

An alcohol-based non-crosslinking tissue fixative, PAXgene Tissue System, has been proposed as alternative fixation method to formalin, providing superior and morphological preservation. To date, metabolites have not been assessed in PAXgene-fixed tissues. The study focuses on a comparison between PAXgene and standard formalin fixation for metabolomic analysis by MALDI mass spectrometry imaging. Therefore, fifty-six samples from seven mice organs were fixed with PAXgene (PFPE) or formalin (FFPE), embedded in paraffin, and processed to a tissue microarray. PAXgene was able to spatially preserve metabolites in organs achieving an overlap of common metabolites ranging from 34 to 78% with FFPE. Highly similar signal intensities and visualization of molecules demonstrated negligible differences for metabolite imaging on PFPE compared to FFPE tissues. In addition, we performed proteomic analysis of intact proteins and peptides derived from enzymatic digestion. An overlap of 33 to 58% was found between FFPE and PFPE tissue samples in peptide analysis with a higher number of PFPE-specific peaks. Analysis of intact proteins achieved an overlap in the range of 0 to 28% owing to the poor detectability of cross-linked proteins in formalin-fixed tissues. Furthermore, metabolite and peptide profiles obtained from PFPE tissues were able to correctly classify organs independent of the fixation method, whereas a distinction of organs by protein profiles was only achieved by PAXgene fixation. Finally, we applied MALDI MSI to human biopsies by sequentially analysing metabolites and peptides within the same tissue section. Concerning prospective studies, PAXgene can be used as an alternative fixative for multi-omic tissue analysis.

Introduction

In the last decade, multi-omic studies have gained enormous traction due to the expectation of a deeper understanding of disease development and progression. The quality of in-depth molecular characterization by modern analytical technologies directly depends on preservation of biomolecules in biological samples. Tissue specimens are usually preserved and stored according to their intended application, either studying histology or the biochemistry of diseases. Formalin fixation and paraffin-embedding (FFPE) is the most widely used technique for tissue stabilization and preservation in routine pathological diagnostics. The tissue fixation with neutral-buffered formalin solution results in the entrapping of biomolecules due to the formation of intra- and intermolecular chemical crosslinks[1]. Primarily, FFPE maintains excellent tissue morphology and works very well in immunohistochemical staining which is important for diagnostic reliability. However, crosslinks between adjacent DNA, RNA, and protein molecules as well as degradation of nucleic acids found in formalin-fixed tissues limit its use in -omics studies. In the last decade, efforts have been made to develop alternative non-crosslinking preservation methods that improve molecular analysis and still enable a traditional pathology testing. Of the commercially available formalin substitutes for tissue fixation[2-6], the PAXgene Tissue System represents one of the best characterized[7-10]. It is based on tissue fixation in a methanol and acetic acid solution, followed by tissue stabilization in ethanol for storage and transportation until samples are embedded in paraffin. In previous studies, PAXgene-fixed and paraffin-embedded (PFPE) tissue specimens, compared to FFPE, have demonstrated to preserve the tissue morphology and antigenicity[9,11,12], while extracted nucleic acids were in quality and quantity improved by PAXgene fixation[10,13,14]. Furthermore, it has been shown that PFPE tissues are amenable to proteomic studies analyzing peptides by liquid chromatography-mass spectrometry (LC-MS)[10], phosphoproteins by western blot and enzyme-linked immunosorbent assay (ELISA)[8], or intact proteins by matrix-assisted laser desorption/ionization mass spectrometry imaging (MALDI-MSI)[7,15].

In the past years, metabolomics has progressed to an important tool in clinical research and the diagnosis of human disease. Using FFPE tissue sections, MALDI Fourier-transform ion cyclotron resonance (FT-ICR) MSI has demonstrated to be a powerful analytical method to determine metabolites in situ[16,17]. To date, metabolomics from PFPE tissue has not been investigated. In this study, we systematically compare PFPE and FFPE mouse tissues to evaluate the potential of PAXgene fixation for metabolite analysis. Additionally, we compared proteomic analysis of intact proteins and peptides derived from enzymatic digestion between PFPE and FFPE tissue specimens. Finally, sequential imaging of metabolites and peptides has been performed for the application on human biopsies.

Material and Methods

Tissue Specimen Collection and Processing

Tissue specimens from two male C57BL/6N littermates at the age of 224 days were dissected after sacrification and independently processed using either 10% neutral-buffered formalin (4% formaldehyde) solution or the PAXgene Tissue System (PreAnalytiX, Hombrechtikon, Switzerland) according to the manufacturer's protocol. Tissues were separately fixed for 18 h in formalin or PAXgene (18 h fixation and 24 h stabilization). Afterwards tissues were dehydrated in graded ethanol, cleared with xylene and embedded in molten paraffin using automated procedures. Generally, formalin-and PAXgene-fixation trap molecular classes within a network of crosslinked (FFPE) or precipitated (PFPE) proteins[18-20].

Tissue Microarray Construction

The tissue microarray (TMA) was assembled from seven organs (heart, kidney, liver, lung, pancreas, spleen, testis) of the two mice (Fig. 1A). With a total of 56 specimens, the TMA contained two tissue cores per organ and fixative (PAXgene, formalin). This formate was chosen as it ensures the very same experimental condition for each of the tissue cores and thus superior comparablility. Animal experiments were in accordance with institutional and national regulations.

Endoscopic Human Biopsies

An overview of the tissue preparation pipeline for human endoscopic biopsies is shown in Fig. 1B. Six endoscopic biopsy particles from two patients, diagnosed with gastro-esophageal adenocarcinoma were collected and fixed in PAXgene according to the manufacturer's protocol or formalin at the University Hospital Essen and the University Medicine Leipzig. The biopsies contained adjacent epithelial and gastric mucosa tissue. The study was approved by the local Ethics Committees.

Tissue Sectioning

Tissue sectioning of the TMA and the human biopsies were performed with a thickness of 4 µm and mounted onto 1:1 (v/v) poly-L-lysine : 0.1% Nonidet P-40 pretreated (Sigma-Aldrich, Munich, Germany) indium-tin-oxide glass slides (Bruker Daltonics, Bremen, Germany).

Metabolite Imaging

Metabolite imaging was performed as previously described for FFPE tissues.[16,17] Briefly, FFPE and PFPE tissue sections were incubated 1 h at 70 °C to allow them to dry and adhere to the slide. Remaining paraffin was removed with xylene (1x8 min, 1x8 min) and thereafter xylene was evaporated at 40 °C. 10 g/l 9-aminoacridine hydrochloride monohydrate matrix (Sigma-Aldrich, Munich, Germany) in 70% methanol was deposited onto the sections using the SunCollect™ sprayer (Sunchrom, Friedrichsdorf, Germany). The first three layers were sprayed with increasing flow rates of 10, 20 and 30 µl/min, while 40 µl/min was used for layers four to eight. MALDI-FT-ICR MSI was

carried out on a Bruker Solarix 7T FTICR MS (Bruker Daltonics), controlled by solariXcontrol (v.1.5.0, Bruker Daltonics) and flexImaging (v.4.0, Bruker Daltonics). Data was acquired in negative ion mode over a mass range of *m/z* 75 - 1,000 with a 1 M data point transient (0.367 s duration) and an estimated resolution of 49,000 at m/z 400. The lateral resolution was set to 60 µm. The Smartbeam-II Nd:YAG (355 nm) laser frequency was set to 1,000 Hz and 100 shots were accumulated per spot. L-arginine was used for external calibration in the ESI mode.

Imaging of Intact Proteins

Protein imaging was performed as previously described for FFPE and PFPE tissues.[7] Briefly, tissue sections were dried and adhered by incubating the slide for 1 h at 70 °C. Remaining paraffin was removed with xylene (2x3 min) and the slides were washed with 2-propanol (3 min). For tissue rehydration, slides were incubated in ethanol dilutions decreasing from 100%, 90%, 70%, 50% to 30% (1 min, each). Following evaporation of ethanol at 40 °C, 10 g/l sinapinic acid matrix (Sigma-Aldrich) in 60% acetonitril / 0.2% trifluoroacetic acid was deposited onto the sections using an ImagePrep automated sprayer (Bruker Daltonics). MALDI-TOF MSI was carried out in linear positive ion mode over a mass range of *m/z* 2,000 - 25,000 using a Bruker Ultraflex III MALDI-TOF/TOF MS (Bruker Daltonics). The lateral resolution was set to 60 µm. The Smartbeam-II Nd:YAG (355 nm) laser frequency was set to 200 Hz with 300 shots per spot and a sample rate of 0.50 GS/s. External calibration was performed with Protein Calibration Standard I (Bruker) mixed 1:1 (v/v) with matrix solution and spotted onto the slide.

Imaging of Digested Proteins (Tryptic Peptides)

Tissue sections were dried and adhered by incubating the slide for 1 h at 70 °C and remaining paraffin was removed with xylene (2x5 min). For tissue rehydration, slides were incubated in ethanol dilutions decreasing from 100% (2x3 min), 70% (1 min) to 30% (1 min), followed by two washing steps in ultrapure water (2x3 min). Antigen retrieval was performed at 97 °C in 10 mM citric acid (pH 6) for 30 min. Thereafter cooled slides were washed for 5 min in ultrapure water and subsequently dried followed by coating with 15 layers of 0.02 µg/µl trypsin gold (Promega, Madison, USA) in ultrapure water at a constant flow rate of 10 µl/min using a SunCollect™ sprayer (Sunchrom). Proteins were digested at 37 °C and 97% humidity for 18 h in a SunDigest™ Incubation Chamber (Sunchrom). 7 g/l α-cyano-4-hydroxycinnamic acid in 50% acetonitrile / 0.2% trifluoroacetic acid were sprayed on the sections using a SunCollect™ sprayer (Sunchrom). The first three layers were sprayed with increasing flow rates of 10, 20 and 30 µl/min, while 40 µl/min was used for layers four to seven. MALDI-TOF MSI was carried out in reflector positive ion mode over a mass range of *m/z* 700 - 4,000 using a Bruker Ultraflex III MALDI-TOF/TOF MS (Bruker Daltonics). The lateral resolution was set to 60 µm. The Smartbeam-II Nd:YAG (355 nm) laser frequency was set to 100 Hz with 200

shots per spot and a sample rate of 2.00 GS/s. External calibration was performed with Peptide Calibration Standard II (Bruker) mixed 1:1 (v/v) with matrix solution and spotted onto the slide.

Sequential Metabolite and Peptide Imaging of Human Endoscopic Biopsies

Metabolite imaging of human endoscopic biopsies was performed according to the protocol used for the mouse TMA. After the measurement, 9-aminoacridine matrix was removed with 70% ethanol for 5 min and sections were further rehydrated, digested and matrix-coated as described in the peptide imaging protocol.

Hematoxylin and Eosin Staining

Following MALDI MSI, the matrix was removed with 70% ethanol for 5 min and sections were stained with hematoxylin and eosin (H&E) as previously described.[17] Stained sections were imaged using a Mirax Desk Scanner (Zeiss, Göttingen, Germany) and co-registered to the MALDI MSI data.

Data Analysis

MALDI-FT-ICR MSI data was exported from flexImaging (v.4.0, Bruker) and analyzed with an in-house developed MATLAB script as previously described[16]. Briefly, data processing included baseline subtraction, smoothing, peak picking, deisotoping and resampling to lower data dimensionality. Peaks which were found in 80% of the samples in each group of organs (e.g. FFPE and PFPE) were picked using a modified version of the LIMPIC algorithm with a minimal peak width of *m/z* 0.0005, an S/N of 2 and an intensity threshold of 0.01%. MALDI-TOF MSI data was exported from flexImaging (v.4.1, Bruker). Further smoothing and peak picking was conducted in mMass (v.5.5.0)[21] using the Savitzky-Golay algorithm (protein spectra: 5 *m/z* window size, 2 cycles; peptide spectra: 0.2 *m/z* window size, 2 cycles) and a S/N of 3 (proteins) or a S/N of 2 with a relative intensity threshold of 0.4 (peptides). Peaks were matched in Mass-up (v.1.0.13)[22] allowing a window of 500 ppm for proteins and 50 ppm for peptides. Hierarchical clustering and heatmap were generated with MetaboAnalyst (v.3.0)[23] using Euclidean distances and the cluster algorithm of Pearson. For this purpose, peaks were picked on the skyline mean spectrum of all tissue specimens and corresponding peak intensities were exported for each tissue core in particular. The comparison of FFPE with PFPE organs was carried out with peaks from the mean spectrum of all tissue cores per organ and fixative. Samples were excluded from data analysis if the tissue core section was lost during H&E staining. Sample numbers of the TMA and human biopsies are listed in Tab. S1. Further data processing was performed with Microsoft Office 2010 (Microsoft Corporation, Redmond, USA) and Prism (v.5.00, GraphPad Software).

Results and Discussion

PAXgene fixation has no adverse effects on the metabolite detection in tissues and enables comprehensive tryptic peptide and intact protein analysis.

To guarantee a high comparability in the analysis of formalin- and PAXgene-fixed tissues a TMA was assembled from seven mouse organs including two independent tissue cores per organ and fixative. Aiming to compare both fixatives, the TMA was measured for metabolites (m/z 100 - 1,000), tryptic peptides (m/z 700 - 4,000) and intact proteins (m/z 3,000 - 25,000). Acquired MALDI MSI spectra of each tissue core were analysed regarding the number, intensity and overlap of peaks in FFPE and PFPE organs (Fig. 2). An organ-independent comparison was performed by combining the data of all FFPE or PFPE tissue cores to a TMA average. Thereby the average number and median intensity of peaks over all PFPE organs (TMA average) in metabolite measurements matched the FFPE samples (Fig. 2A,C) and 56.2% of the peaks were found to be identical between both fixation procedures (Fig. 2B). In dependency on the fixation method, a proportion of metabolites were more amenable for MALDI-MSI analysis than others, leading to 18.3% FFPE- and 25.9% PFPE-specific m/z species (Fig. 2B). In contrast, 56.2% of all peaks were detectable in FFPE and PFPE tissues and thus irrespective of the fixation type. There are several aspects of chemistry that have not yet been fully understood regarding the modification of molecular species, particularly metabolites, in fixed tissues. A number of mass spectrometry metabolic studies demonstrated that most metabolites, with the exception of lipids, are conserved in FFPE tissues without changes[16,24-26]. The processes of tissue embedding and removal of paraffin wax via solvents reduce the detection of lipid species by MALDI MSI although fatty acids and some solvent-resistant lipids are retained[16]. Another study reported that lipid species might undergo peroxidation or oxidation in FFPE brain tissue[27]. Otherwise, it is assumed that solvent-only preservatives compared to formalin fixation lead to less or no chemical modifications as demonstrated for proteins and nucleic acids[8,10,13,28].

The measurement of digested proteins (tryptic peptides) revealed a slight increase in the amount of peaks detected in PFPE tissues with a reduced overlap of 47.6% between FFPE and PFPE (Fig. 2D,E). Likewise metabolite imaging, median signal intensities of PFPE peptide peaks matched the corresponding peaks in formalin-fixed tissues (Fig. 2F). The analysis of intact proteins, as compared to peptide and metabolite imaging, revealed an overall decreasing amount of *m/z* species in PFPE and FFPE tissues but with consistently higher numbers of PFPE-specific peaks (Fig. 2G). In addition, intact protein measurements revealed the lowest percentage of overlapping *m/z* species (Fig 2H). As expected, protein peak numbers and peak intensities of PAXgene-fixed tissues were found to be higher across all organs (Fig 2I), which is in line with previous findings of Ergin et al.[7]. In conclusion, the highest molecular overlap was achieved in the analysis of metabolites, while PAXgene-fixed

tissues tend to rise output of peptides. The strongest differences were found in the analysis of intact proteins with a significantly improved detection of proteins in PAXgene-fixed tissue samples.

Molecular imaging of intact proteins from FFPE tissue samples strongly impaired the spectra quality (e.g. signal intensity, S/N ratio, mass range), as illustrated by the mean spectra from pancreatic tissue (Fig. 3A). The PFPE spectrum displayed a multitude of peaks with higher signal intensities (Fig. 3A). As an example, insulin with m/z 5,805 detected from PFPE co-localized with the islet of Langerhans which was already shown in earlier MSI studies (Fig. 3B)[7,29]. Despite the much poorer spectra quality, insulin was also detectable from FFPE pancreatic tissue with m/z 5,827 (Fig. 3C), but with lower signal intensity (Fig. 3A,D). An extraction of mass spectrometric profiles from the islet of Langerhans revealed differences between the insulin pattern obtained from PFPE and FFPE tissue (Fig. 3D). A pattern of three m/z species with m/z 5,813, m/z 5,827 and m/z 5,839, was obtained from the FFPE islet of Langerhans. The formation of the peak pattern is related to the process of formalin fixation as reported by Metz et al.[18,19]. Nucleophilic N-terminal amino groups as well as amino and thiol side chain groups of various amino acids react with formaldehyde by introducing unstable methylol groups (-CH_2OH). Subsequent dehydration of methylol groups on lysine and tryptophan residues enables the formation of Schiff bases. Especially Schiff base-modified lysine side chains were found to react with further amino acids by forming stable methylene (-CH_2-) crosslinks. Additionally, N-terminal amino groups cycle via Schiff base intermediates to 4-imidazolidinone adducts[19]. Consequently, formaldehyde induces mass shifts by intra- or intermolecular methylene crosslinks (-NH-**CH_2**-NH-, +12 Da) and amino acid modifications with methylol (-NH-**CH_2OH**, +30 Da), methyl (lysine-NH-**CH_3**, +14 Da) and Schiff base (-N**=CH_2**, +12 Da) adducts[19,30]. In the FFPE spectrum the three insulin-related peaks revealed mass differences of Δm/z 14 and Δm/z 12, which indicated the presence of some of the previously mentioned modifications: methylated lysine, Schiff base adducts, or intramolecular methylene bridges. According to Metz et al.[18,19], not all theoretically nucleophilic amino acids react with formaldehyde when using native proteins instead of model peptides. The tendency of forming adducts and crosslinks is rather determined by the intrinsic reactivity and accessibility of each amino acid in the folded protein[18]. Applying these findings to our observations in FFPE tissue, it is likely that insulin only partly reacted with formalin and therefore was still accessible for MALDI analysis. Based on insulin as example, peaks in FFPE tissues represent various formalin-modified species of the same protein or peptide, each with different m/z. In contrast, PAXgene-fixed tissues lack any fixative-mediated covalent protein modifications and the usual peak shape was observed.

Organ-specific comparison of peak numbers and overlaps between FFPE and PFPE tissues.

Subsequently we investigated the number and proportion of m/z species by comparing each FFPE and PFPE organ of the TMA in the data of metabolites, peptides and proteins. A comparison of the m/z overlap, found between FFPE and PFPE, displays that metabolite spectra of the heart, lung and kidney had more than 65% of matching peaks followed by liver, spleen and testis with more than 45% (Fig. 4A). Solely PAXgene-fixed pancreatic tissues differed by increasing amounts of PFPE-specific peaks between m/z 400 and 1,000. Peaks detected in peptide measurements (Fig. 4B) consistently overlapped between 32.7% (spleen) to 57.5% (lung), whereas protein spectra (Fig. 4C) showed the lowest percentage of matching FFPE and PFPE peaks between 0% (heart) and 27.6% (pancreas). These findings especially demonstrated the potential of PFPE for intact protein analysis by MALDI MSI. Generally, the organ-specific analysis of spectra from PFPE tissues further highlighted the functionality of PAXgene fixation across all organs of the TMA. The reduced detection of metabolite m/z species in the higher mass range (m/z 600 - 1000) is mainly attributed to lipid loss by solvents during the tissue embedding process or paraffin removal[16,31], while it has been shown that the lipid content is not markedly affected by formalin fixation itself[31]. Therefore the analysis of lipids in alcohol- or formalin fixed and paraffin-embedded tissues is not the first choice according to the current literature[17,31].

Taking the spleen as exemplary organ (Fig. 5), the overall findings of Fig. 2 and 4 are shown in an organ-specific manner. Again, metabolite imaging of both fixation methods revealed the highest number and overlap of m/z species with 48.0% (Fig. 5A,B,C), followed by tryptic peptide (Fig. 5F,G,H) and intact protein (Fig. 5K,L,M) measurements with 32.7% and 14.9%, respectively. Exclusively metabolite spectra of the spleen revealed 121 m/z species which were equally abundant in the different fixed tissues and almost twice as much m/z species with higher intensities in PFPE samples (Fig. 5D). In the peptide analysis was an overlap of 187 m/z equal abundant species between PFPE and FFPE spleen and only 16 m/z species were higher or 2 lower in PFPE (Fig. 5I). The differences in signal intensities lead to images of certain metabolites (Fig. 5E) and peptides (Fig. 5J) missed in PFPE (e.g. m/z 348.668 and m/z 2476.49) or FFPE (e.g. m/z 290.883 and m/z 3238.84) tissues. Nevertheless, PAXgene was able to spatially preserve the majority of metabolites and peptides in a similar way to FFPE fixation as exemplified by m/z 160.842 for metabolites and m/z 1529.96 for peptides (Fig. 5E,J). Analysing intact proteins the PAXgene fixation significantly increased signal abundances (Fig. 5N). A precise assignment of proteins to tissue features was achieved for PFPE spleen, as illustrated for m/z 11,334 co-localizing with the white pulp, while no adequate image could be obtained from FFPE spleen (Fig. 5O). This observation was in line with previous studies demonstrating that formalin-induced protein crosslinks highly decreased the number and intensity of peaks and, in general, rule out proper protein images from FFPE tissues by MALDI MSI[7,32].

In another study, comparable numbers of tryptic peptides were found between PFPE and FFPE samples using LC-MS/MS analysis[10]. Additionally, the same percentage of peptides was assigned to protein identities[10]. Although MALDI MSI found that the majority of peptides visualizable in FFPE spleen could also be visualized in PFPE, a fraction of images was specific for FFPE or PFPE (Fig. 5J). Based upon the nature of fixative, formalin fixation and antigen retrieval lead to chemical modifications and molecular differences between FFPE and PFPE tissues[18,19,33].

Classification of organs is independent of the fixation method for metabolites and peptides.

Spectra from PFPE tissues were compared to FFPE tissues using quantitative properties such as peak numbers and signal intensities. However, one important application of MALDI MSI is the analysis of various tissues to identify tissue- and disease-specific molecular patterns. Therefore, we compared the quality of data from metabolite, peptide and protein measurements in terms of their ability to separate organs into different groups by hierarchical cluster analysis. Given that formalin or PAXgene fixation has a predominant effect on the detection of organ-specific m/z species, hierarchical clustering would fail to assign each tissue core to its corresponding organ. Consequently, variations due to different fixation methods would be higher than actual biological variations and mainly two clusters are generated, one for FFPE and one for PFPE tissues. As expected, the 50 most discriminating m/z species of metabolite and peptide measurements successfully identified the origin of each tissue core (Fig. 6A,B). The hierarchical cluster analysis and heatmap of metabolite and peptide analyses highlight an fixation-independent seperation of organs. In contrast, by using protein data, classification was dependent on the fixation method. Thereby the cluster tree divided into FFPE and PFPE clusters at the very first branch (Fig. 6C). Further clustering of the PFPE group with protein peaks achieved an almost perfect distinction of organs except of a single outlier of a testis tissue core. The clustering of FFPE tissues, however, did not result in organ-specific groups which was mainly attributed to the poor spectral quality with a low number of peaks in protein measurements (Fig. 6C, Fig. 4C). These results demonstrated that PAXgene highly preserves tissue-specific information for metabolites, peptides, and proteins which is necessary to address comprehensive biological questions.

Analysis of human biopsies by sequential metabolite and peptide imaging

The suitability of PFPE tissues for metabolite and peptide measurements of mouse organs was demonstrated in this study. Although the TMA represents an idealized and highly comparable research format, the performance of MALDI imaging on actual PFPE patient material is crucial for tissue based diagnostics and research. Therefore, we imaged human biopsies that represent one of the most important and challenging tissue materials: important due to the high value of biopsies in

accurate diagnosis and pre-therapeutic decision making and challenging because of the restricted amount of tissue available for molecular testing. To substantially increase the molecular information from the very same tissue section, either formalin- or PAXgene-fixed biopsy particles were sequentially measured for metabolites and peptides. Thereby, biopsy tissue sections remained intact during metabolite and peptide MALDI MSI analyses which enabled the co-registration of MALDI MSI data to histologically stained sections. In this context, both fixation methods revealed peaks co-localizing with histological features such as squamous epithelium and tumor tissue (Fig. 7A,B). Comparable to prior metabolite measurements of the TMA, a similar number of m/z species between formalin- and PAXgene-fixed biopsies was found (Fig. 7C). In the peptide analysis, the trend towards higher peak numbers was more pronounced in PFPE human biopsy tissue samples (Fig. 7D).

Conclusion

This is the first study addressing metabolomic analysis from PFPE tissue samples. Our analysis of tissue specimens processed by the PAXgene Fixation System yielded a similar coverage of metabolites with highly comparable peak numbers and intensities to FFPE. In addition, proteomic analysis was performed using MALDI MSI. Imaging of peptides derived from enzymatic digestion were slightly more amenable from PFPE than FFPE tissue sections with a trend towards increased peak numbers. By contrast, the analysis of intact proteins benefitted considerably in the spectral quality when using PAXgene instead of formalin-fixed tissue samples. Previous findings indicated a number of molecular classes, e.g. DNA, RNA, microRNA and proteins, which are better detectable after PAXgene fixation. In our comparison, the PAXgene-fixation demonstrated indeed an improved detection of intact proteins by MALDI MSI. However, similar results were achieved by imaging metabolites and tryptic peptides from PFPE and FFPE tissue. The PAXgene Tissue System preserved well tissue-specific information for metabolites, peptides, and proteins allowing a successful classification of tissue cores in an organ dependent manner using hierarchical cluster analysis. Further we showed that the sequential testing of metabolites and tryptic peptides from the same tissue section increase the molecular information from FFPE and PFPE tissue sections by using MALDI MSI, which can be useful in resource-limiting settings, in particular of limited available tissue from endoscopic biopsies.

Author Contributions

C.U. and A.B. carried out experiments, performed the statistical analysis, interpreted the results and wrote the manuscript. J.T.S., F.L. and B.L. provided human material and edited the manuscript. A.W. designed the study, interpreted results and wrote the manuscript. M.A. designed the study and wrote the manuscript.

Acknowledgments

A.W. was funded by the Ministry of Education and Research of the Federal Republic of Germany (BMBF; Grant Nos. 01ZX1310B, 01KT16015), the Deutsche Forschungsgemeinschaft (Grant Nos. SFB 824 TP Z02 / C4, CRC/TRR 205 S01) and the Deutsche Krebshilfe (No. 70112617). We thank Ulrike Buchholz, Claudia-Mareike Pflüger, Gabriele Mettenleiter, and Andreas Voss for excellent technical assistance.

(1) Renshaw, S. *Immunochemical Staining Techniques.*; Scion Publishing Ltd: Bloxham, UK, 2007; Vol. Ch. 4.
(2) Dotti, I.; Bonin, S.; Basili, G.; Nardon, E.; Balani, A.; Siracusano, S.; Zanconati, F.; Palmisano, S.; De Manzini, N.; Stanta, G. *Diagnostic molecular pathology : the American journal of surgical pathology, part B* **2010**, *19*, 112-122.
(3) Delfour, C.; Roger, P.; Bret, C.; Berthe, M. L.; Rochaix, P.; Kalfa, N.; Raynaud, P.; Bibeau, F.; Maudelonde, T.; Boulle, N. *The Journal of molecular diagnostics : JMD* **2006**, *8*, 157-169.
(4) Olert, J.; Wiedorn, K. H.; Goldmann, T.; Kuhl, H.; Mehraein, Y.; Scherthan, H.; Niketeghad, F.; Vollmer, E.; Muller, A. M.; Muller-Navia, J. *Pathology, research and practice* **2001**, *197*, 823-826.
(5) Stanta, G.; Mucelli, S. P.; Petrera, F.; Bonin, S.; Bussolati, G. *Diagnostic molecular pathology : the American journal of surgical pathology, part B* **2006**, *15*, 115-123.
(6) Viertler, C.; Groelz, D.; Gündisch, S.; Kashofer, K.; Reischauer, B.; Riegman, P. H. J.; Winther, R.; Wyrich, R.; Becker, K.-F.; Oelmüller, U.; Zatloukal, K. *The Journal of Molecular Diagnostics* **2012**, *14*, 458-466.
(7) Ergin, B.; Meding, S.; Langer, R.; Kap, M.; Viertler, C.; Schott, C.; Ferch, U.; Riegman, P.; Zatloukal, K.; Walch, A.; Becker, K. F. *Journal of proteome research* **2010**, *9*, 5188-5196.
(8) Gundisch, S.; Schott, C.; Wolff, C.; Tran, K.; Beese, C.; Viertler, C.; Zatloukal, K.; Becker, K. F. *PloS one* **2013**, *8*, e60638.
(9) Kap, M.; Smedts, F.; Oosterhuis, W.; Winther, R.; Christensen, N.; Reischauer, B.; Viertler, C.; Groelz, D.; Becker, K. F.; Zatloukal, K.; Langer, R.; Slotta-Huspenina, J.; Bodo, K.; de Jong, B.; Oelmuller, U.; Riegman, P. *PloS one* **2011**, *6*, e27704.
(10) Mathieson, W.; Marcon, N.; Antunes, L.; Ashford, D. A.; Betsou, F.; Frasquilho, S. G.; Kofanova, O. A.; McKay, S. C.; Pericleous, S.; Smith, C.; Unger, K. M.; Zeller, C.; Thomas, G. A. *American journal of clinical pathology* **2016**, *146*, 25-40.
(11) Belloni, B.; Lambertini, C.; Nuciforo, P.; Phillips, J.; Bruening, E.; Wong, S.; Dummer, R. *Journal of clinical pathology* **2013**, *66*, 124-135.
(12) Gundisch, S.; Slotta-Huspenina, J.; Verderio, P.; Ciniselli, C. M.; Pizzamiglio, S.; Schott, C.; Drecoll, E.; Viertler, C.; Zatloukal, K.; Kap, M.; Riegman, P.; Esposito, I.; Specht, K.; Babaryka, G.; Asslaber, M.; Bodo, K.; den Bakker, M.; den Hollander, J.; Fend, F.; Neumann, J.; Reu, S.; Perren, A.; Langer, R.; Lugli, A.; Becker, I.; Richter, T.; Kayser, G.; May, A. M.; Carneiro, F.; Lopes, J. M.; Sobin, L.; Hofler, H.; Becker, K. F. *Virchows Archiv : an international journal of pathology* **2014**, *465*, 509-519.
(13) Andersen, G. B.; Hager, H.; Hansen, L. L.; Tost, J. *Analytical biochemistry* **2015**, *468*, 50-58.
(14) Groelz, D.; Sobin, L.; Branton, P.; Compton, C.; Wyrich, R.; Rainen, L. *Experimental and molecular pathology* **2013**, *94*, 188-194.
(15) Oetjen, J.; Aichler, M.; Trede, D.; Strehlow, J.; Berger, J.; Heldmann, S.; Becker, M.; Gottschalk, M.; Kobarg, J. H.; Wirtz, S.; Schiffler, S.; Thiele, H.; Walch, A.; Maass, P.; Alexandrov, T. *Journal of proteomics* **2013**, *90*, 52-60.
(16) Buck, A.; Ly, A.; Balluff, B.; Sun, N.; Gorzolka, K.; Feuchtinger, A.; Janssen, K. P.; Kuppen, P. J.; van de Velde, C. J.; Weirich, G.; Erlmeier, F.; Langer, R.; Aubele, M.; Zitzelsberger, H.; Aichler, M.; Walch, A. *The Journal of pathology* **2015**, *237*, 123-132.
(17) Ly, A.; Buck, A.; Balluff, B.; Sun, N.; Gorzolka, K.; Feuchtinger, A.; Janssen, K. P.; Kuppen, P. J.; van de Velde, C. J.; Weirich, G.; Erlmeier, F.; Langer, R.; Aubele, M.; Zitzelsberger, H.; McDonnell, L.; Aichler, M.; Walch, A. *Nature protocols* **2016**, *11*, 1428-1443.
(18) Metz, B.; Kersten, G. F.; Baart, G. J.; de Jong, A.; Meiring, H.; ten Hove, J.; van Steenbergen, M. J.; Hennink, W. E.; Crommelin, D. J.; Jiskoot, W. *Bioconjugate chemistry* **2006**, *17*, 815-822.
(19) Metz, B.; Kersten, G. F.; Hoogerhout, P.; Brugghe, H. F.; Timmermans, H. A.; de Jong, A.; Meiring, H.; ten Hove, J.; Hennink, W. E.; Crommelin, D. J.; Jiskoot, W. *The Journal of biological chemistry* **2004**, *279*, 6235-6243.
(20) van Essen, H. F.; Verdaasdonk, M. A.; Elshof, S. M.; de Weger, R. A.; van Diest, P. J. *Journal of clinical pathology* **2010**, *63*, 1090-1094.
(21) Strohalm, M.; Kavan, D.; Novák, P.; Volný, M.; Havlíček, V. *Analytical chemistry* **2010**, *82*, 4648-4651.

(22) López-Fernández, H.; Santos, H. M.; Capelo, J. L.; Fdez-Riverola, F.; Glez-Peña, D.; Reboiro-Jato, M. *BMC Bioinformatics* **2015**, *16*, 318.
(23) Xia, J.; Wishart, D. S. In *Current Protocols in Bioinformatics*; John Wiley & Sons, Inc., 2002.
(24) Kelly, A. D.; Breitkopf, S. B.; Yuan, M.; Goldsmith, J.; Spentzos, D.; Asara, J. M. *PloS one* **2011**, *6*, e25357.
(25) Wojakowska, A.; Marczak, L.; Jelonek, K.; Polanski, K.; Widlak, P.; Pietrowska, M. *PloS one* **2015**, *10*, e0136902.
(26) Cacciatore, S.; Zadra, G.; Bango, C.; Penney, K. L.; Tyekucheva, S.; Yanes, O.; Loda, M. *Molecular cancer research : MCR* **2017**, *15*, 439-447.
(27) Hackett, M. J.; McQuillan, J. A.; El-Assaad, F.; Aitken, J. B.; Levina, A.; Cohen, D. D.; Siegele, R.; Carter, E. A.; Grau, G. E.; Hunt, N. H.; Lay, P. A. *The Analyst* **2011**, *136*, 2941-2952.
(28) Chaurand, P.; Latham, J. C.; Lane, K. B.; Mobley, J. A.; Polosukhin, V. V.; Wirth, P. S.; Nanney, L. B.; Caprioli, R. M. *Journal of proteome research* **2008**, *7*, 3543-3555.
(29) Green-Mitchell, S. M.; Cazares, L. H.; Semmes, O. J.; Nadler, J. L.; Nyalwidhe, J. O. *Proteomics. Clinical applications* **2011**, *5*, 448-453.
(30) Zhang, Y.; Muller, M.; Xu, B.; Yoshida, Y.; Horlacher, O.; Nikitin, F.; Garessus, S.; Magdeldin, S.; Kinoshita, N.; Fujinaka, H.; Yaoita, E.; Hasegawa, M.; Lisacek, F.; Yamamoto, T. *Proteomics* **2015**, *15*, 2568-2579.
(31) Pietrowska, M.; Gawin, M.; Polańska, J.; Widłak, P. *Proteomics* **2016**, *16*, 1670-1677.
(32) Lemaire, R.; Desmons, A.; Tabet, J. C.; Day, R.; Salzet, M.; Fournier, I. *Journal of proteome research* **2007**, *6*, 1295-1305.
(33) Djidja, M. C.; Claude, E.; Scriven, P.; Allen, D. W.; Carolan, V. A.; Clench, M. R. *Biochimica et biophysica acta* **2016**.

Figure 1. Mass spectrometry imaging workflow for the analysis of metabolites (MALDI-FT-ICR MSI), tryptic peptides and intact proteins (MALDI-TOF MSI). (A) Mouse organs were either formalin- or PaxGene-fixed, paraffin-embedded, and arranged in a tissue microarray. (B) Human biopsy particles, either formalin- or PaxGene-fixed, and paraffin-embedded were sequentially analyzed for metabolites and peptides.

Figure 2. Metabolite, tryptic peptide and intact protein measurements of FFPE and PFPE mouse TMA specimens were compared regarding the number, overlap and intensity of m/z species. (A, D, G) Mean number of m/z species in FFPE and PFPE tissues with standard deviations determined for each mouse organ (heart, kidney, liver, lung, pancreas, spleen, testis). The TMA average was calculated using the number of m/z species for each tissue core of the TMA. (B, E, H) Venn diagrams highlight the mean proportional overlap of FFPE and PFPE peaks with standard deviations based on seven mouse organs. (C, F, I) Box-Whisker plots show the logarithmic signal intensity ratio of PFPE peaks, normalized to the corresponding FFPE peaks. Signal intensity ratios of all seven organs were considered for the TMA average. Peak intensities for each organ were taken from the mean spectrum which included all tissue cores per organ and fixation method.

Figure 3. Imaging of undigested insulin in mouse pancreatic tissues of the TMA. (A) Mean spectrum of the FFPE and PFPE pancreatic tissue core. (B, C) FFPE and PFPE tissue cores showing the co-localization of insulin with the islet of Langerhans at m/z 5,827 or m/z 5,805. (D) Islet of Langerhans-specific spectra for FFPE and PFPE specimen.

Figure 4. Organ-specific comparison of peak numbers and overlaps between FFPE and PFPE tissues. Metabolite (A), peptide (B) and protein (C) measurements of all mouse tissue specimens of the TMA. Data analysis is based on the organ-specific mean spectrum of FFPE and PFPE samples. The total number of m/z species is given for the m/z range 100 to 1,000 with an interval size of m/z 100 for metabolites, in the m/z range 700 to 4,000 with an interval size of m/z 330 for peptides, and in the m/z range 3,000 to 25,000 with an interval size of m/z 2,000 for proteins. Additonal Venn diagrams show the percentage of matching and non-matching FFPE and PFPE peaks.

Figure 5. Metabolite, peptide, and protein measurements of mouse spleen tissue specimens. Data analysis is based on the mean spectrum of four FFPE or PFPE tissue samples. (A, F, K) Mean spectra of FFPE and PFPE tissue specimens. (C, H, M) Venn diagrams show the total number and percentage of matching and non-matching FFPE and PFPE peaks. (B, G, L) Total number of m/z species in the m/z range 100 to 1,000 with an interval size of m/z 100 for metabolites, in the m/z range 700 to 4,000 with an interval size of m/z 330 for peptides, and in the m/z range 3,000 to 25,000 with an interval size of m/z 2,000 for proteins. (D, I, N) Number of overlapping m/z species in FFPE and PFPE samples, classified according to their signal intensity. Therefore, PFPE peak intensities were normalized to corresponding FFPE peaks and the intensity of PFPE peaks was classified as lower ($I_{PFPE}/I_{FFPE} < 0.5$), equal ($0.5 < I_{PFPE}/I_{FFPE} < 2.0$), or higher ($2.0 < I_{PFPE}/I_{FFPE}$) compared to FFPE peaks. (E, J, O) Exemplary visualization of m/z species which were found to be more or equally abundant in FFPE or PFPE tissue specimen.

Figure 6. Hierarchical clustering and heatmap of single FFPE and PFPE tissue cores against each organ of the TMA for metabolite, peptide and protein measurements. Each class is defined by an organ and Euclidean distances were used in combination with the cluster algorithm of Pearson. Using the 50 most significant m/z species, metabolite (A) and peptide (B) profiles obtained from FFPE and PFPE tissues lead unambiguously to an organ dependent clustering independent of the fixation method. In contrast, classification using protein data (C) separated the organs depend on the fixation method into FFPE or PFPE clusters. PFPE tissues further enabled an organ dependent assignment of tissues which was impossible with FFPE protein profiles.

Figure 7. Sequential metabolite and peptide imaging of human FFPE and PFPE biopsies. (A,B) Visualization of six m/z species which co-localize with histological properties, e.g. squamous epithelium and tumor tissue. (C,D) Mouse TMA and human biopsy specimens were compared according to the mean number of m/z species with standard deviations determined for each mouse tissue core (n=28 for FFPE samples, n=26 for PFPE samples) or human biopsy particle (n=6) and mean spectra of all six biopsy particles for each fixation method.

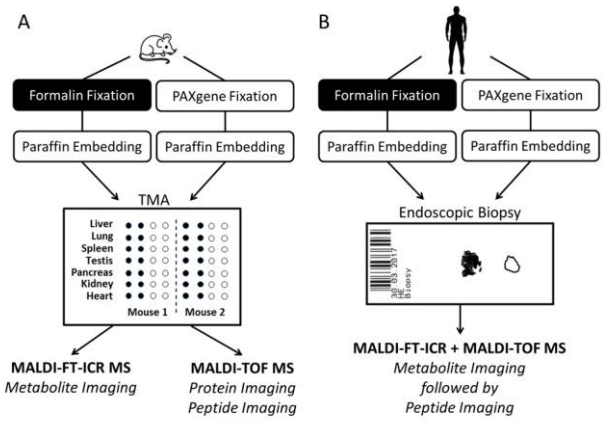

Figure 1

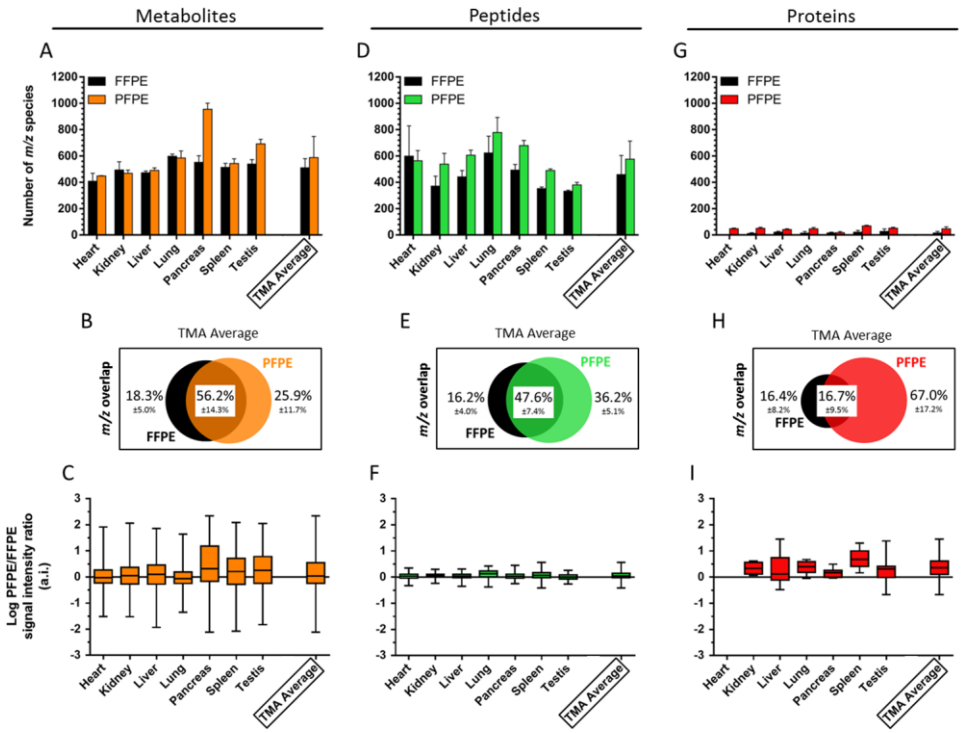

Figure 2

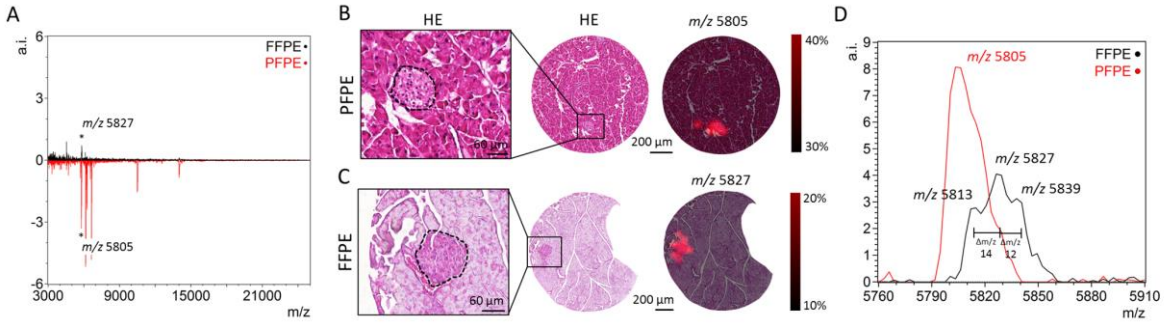

Figure 3

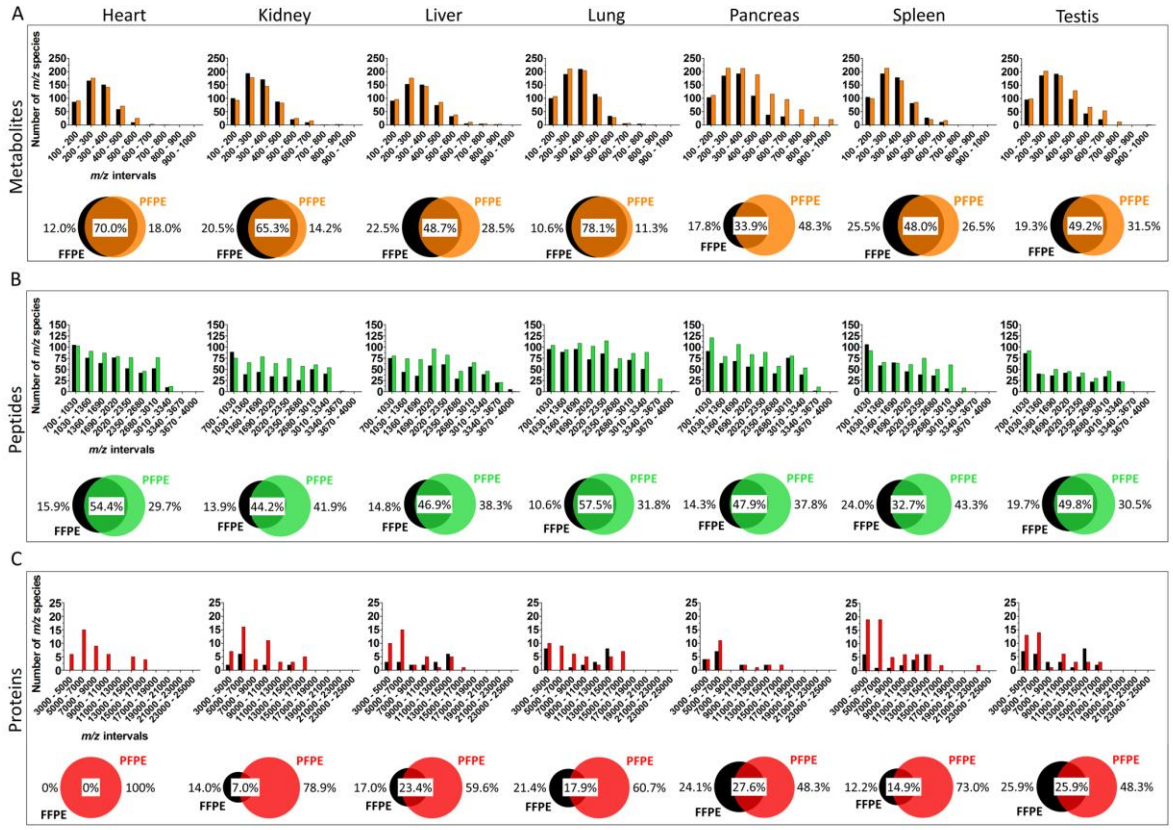

Figure 4

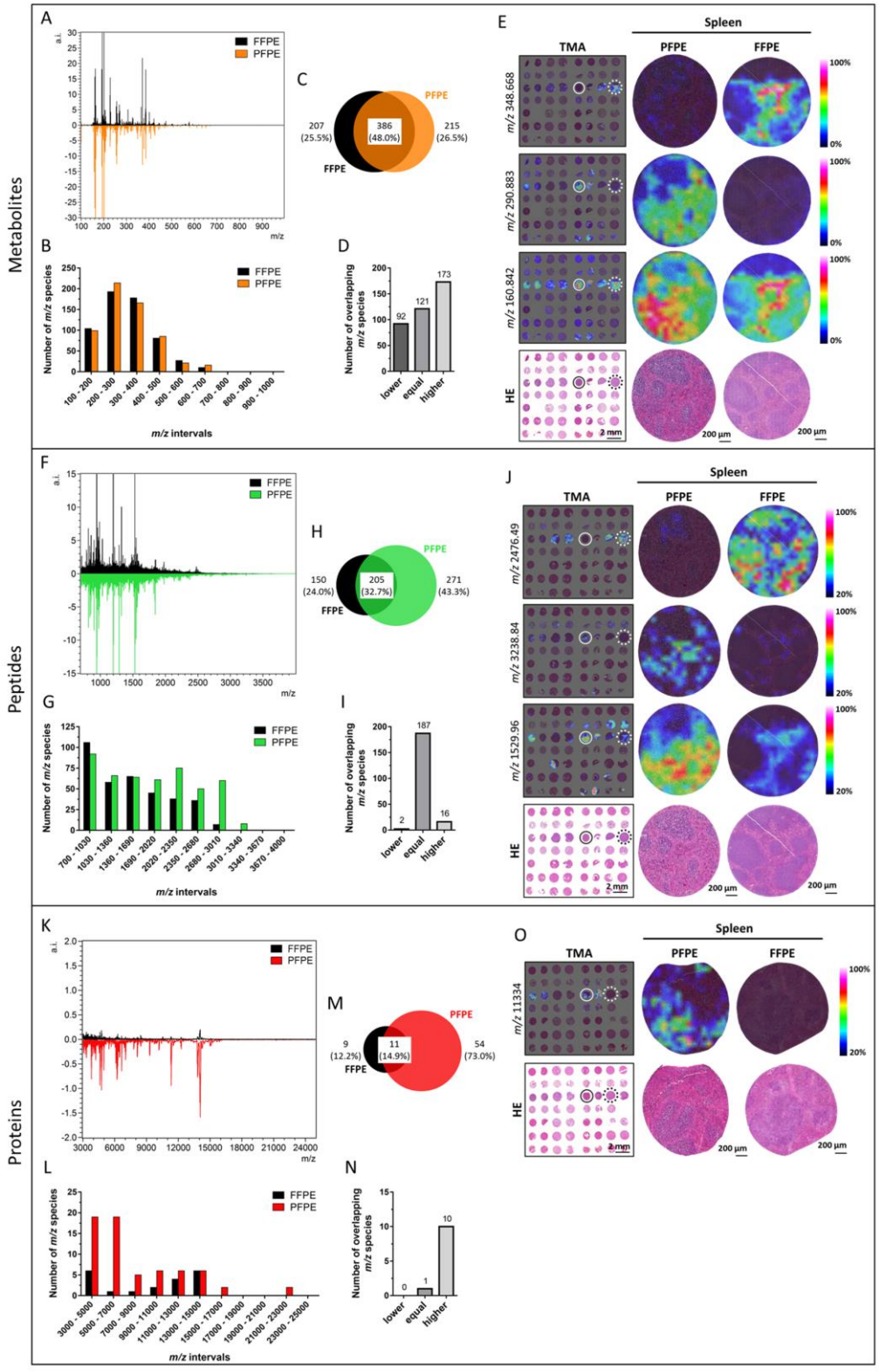

Figure 5

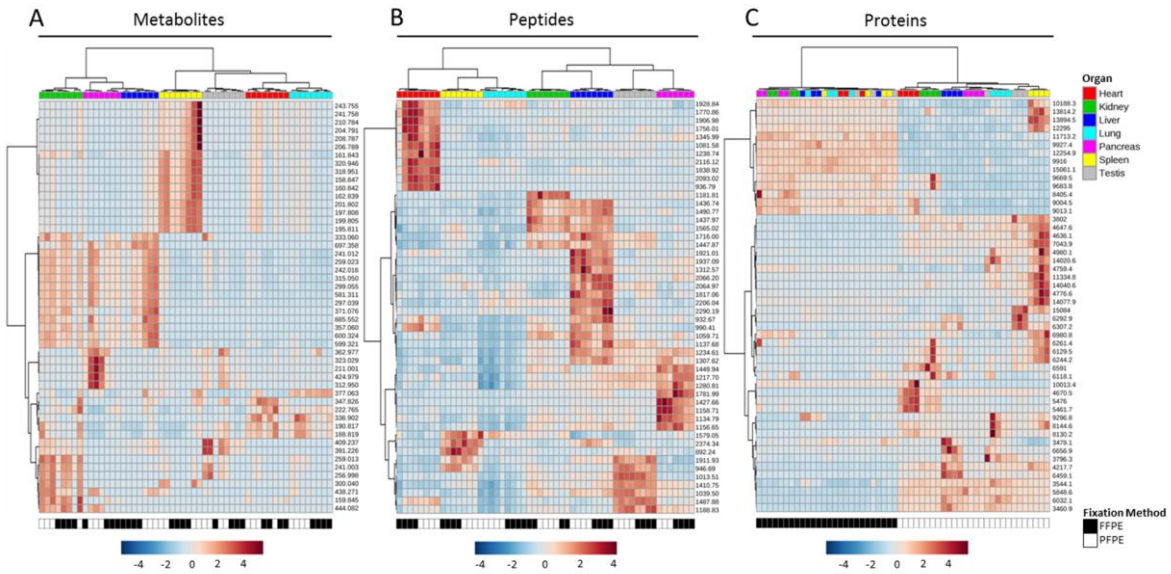

Figure 6

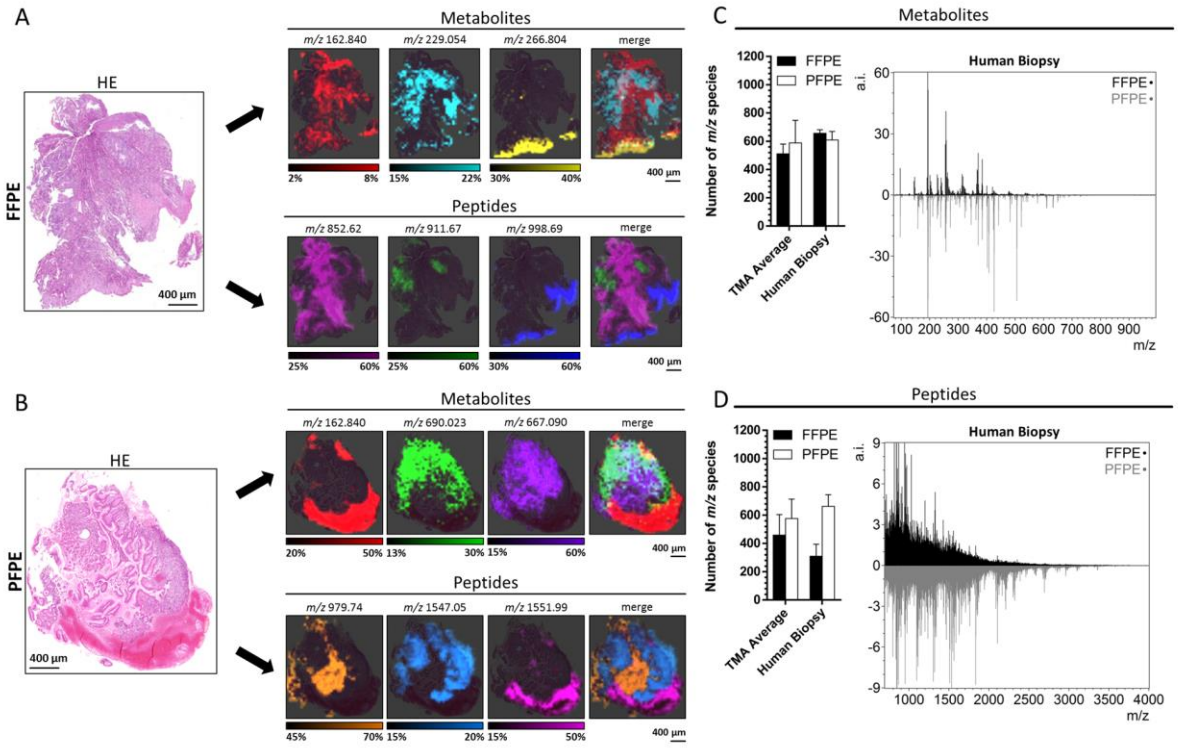

Figure 7

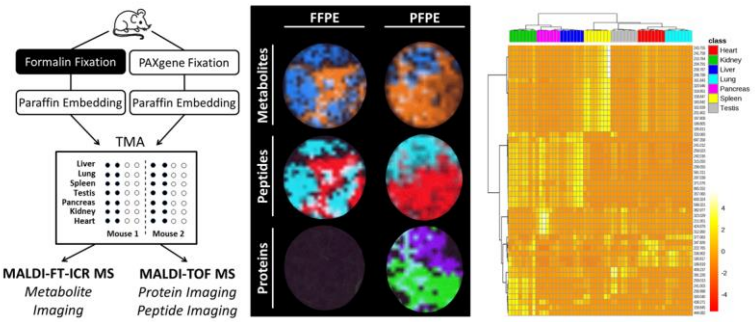

Graphical abstract

Highlights

- an alcohol-based non-crosslinking tissue fixative, PAXgene Tissue System, is proposed as an alternative fixation method for metabolomic and proteomic tissue analyses
- a systematic comparison between PAXgene-fixed and formalin-fixed and paraffin-embedded tissue samples was performed by MALDI mass spectrometry imaging
- PAXgene fixation yield similar coverage in metabolite and peptide analyses while detection of intact proteins is improved in PAXgene compared to formalin-fixed tissues